M&C 2017 - International Conference on Mathematics & Computational Methods Applied to Nuclear Science & Engineering, Jeju, Korea, April 16-20, 2017, on USB (2017)

Automated ADVANTG Variance Reduction in a Proton Driven System

Kenneth A. Van Riper[1] and Robert L. Metzger[2]

[1]*White Rock Science, P. O. Box 4729, White Rock, NM 87547, kvr@rt66.com*
[2]*Radiation Safety Engineering, 3245 N. Washington, Chandler, AZ 85225, rlmetzger@radsafe.com*

Abstract – *We discuss the use of the ADVANTG automated variance reduction program for shielding studies of a vault containing targets irradiated by cyclotron accelerated protons. Because ADVANTG is limited to neutron and photon models, our calculations proceeded in several steps. Neutrons and photons emanating from a sphere surrounding the target were saved to a surface source file. This file was used to define sources for the ADVANTG runs and as a source for subsequent Monte Carlo runs. Test runs were made to ensure the validity of each step. The final calculations using the ADVANTG produced weight windows ran much more quickly and gave the same results as a model using only importance splitting for variance reduction.*

I. INTRODUCTION

We recently completed a shielding design for a cyclotron vault on the Mayo Clinic's Scottsdale, AZ campus [1]. That work used Monte Carlo calculations by MCNPX, version 2.7 [2] to evaluate the neutron and photon transport through the 1.83 m (6') thick concrete walls and ceiling and streaming through the entrance maze. Variance reduction is required to calculate penetration of the thick concrete barriers and to direct the radiation through the maze. We used the technique of importance splitting with 26 importance layers through the walls and 31 layers between the source and the entrance.

More recently, we were commissioned to evaluate the shielding of a similar cyclotron vault. For this work, we used the MCNP6, version 6.1 [3] Monte Carlo code and the ADVANTG [4] code to calculate Weight Windows (WWs) to be used for variance reduction. Because ADVANTG is only applicable to neutron and photon transport and not to the cyclotron's proton beam impinging on a target, several steps were necessary. In the first stage, the neutrons and photons crossing a sphere surrounding the target were written to an MCNP surface source (SS) file. Neutron and photon tallies on that sphere were converted to sources for the ADVANTG calculations. The resulting neutron and photon weight windows were merged and used in the final MCNP6 runs with the surface source read (SSR) feature. A number of test calculations were made to check the validity of some approximations and to resolve a discrepancy initially found between the MCNP6 and MCNPX results.

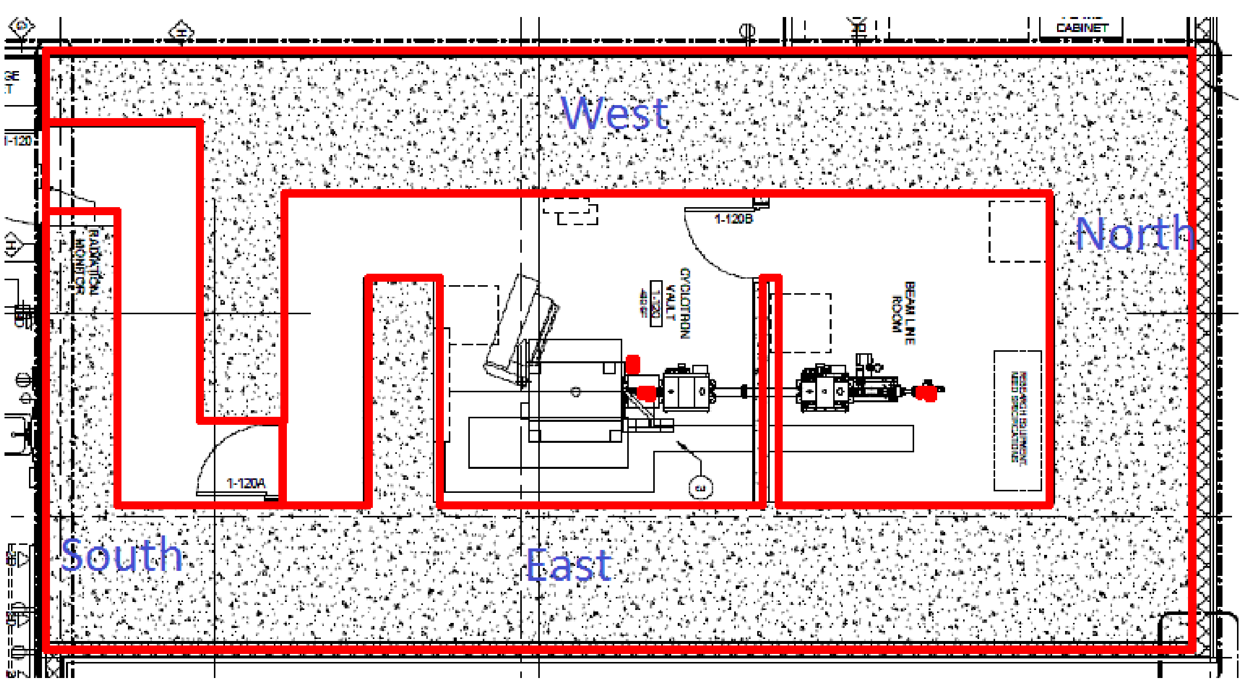

Fig. 1. Monte Carlo model (red) overlaid on architectural drawing.

II. DESCRIPTION OF THE ACTUAL WORK

1. Cyclotron Vault Model

The vault houses a General Electric cyclotron. The primary use is production of ^{18}F for PET imaging. The PET isotopes are produced in a target adjacent to the accelerator. The proton beam can be directed to an external target in an adjoining room for production of other clinical and research isotopes including ^{11}C, ^{13}N, ^{15}O, ^{63}Zn, and ^{68}Ga. We refer to the former as the *cyclotron target* and the latter as the *external target*.

A. Geometry

Figure 1 shows a floor plan of the model overlaid on an architectural drawing of the building. Thick red lines outline the Monte Carlo regions except for the interior and exterior air spaces. From south to north (left to right in Fig. 1), the model consists of the entrance maze, the cyclotron room containing the cyclotron target and collimator material, and the external target room with the external target. Also shown in red are the outlines of the targets and the collimator. The concrete walls and ceiling are 1.83 m (6') thick. The ceiling height within the vault is 3.048 m (10”). The concrete floor is 0.9144 m (3”) thick. An air space approximately 1.1 m (3 ½”) thick surrounds the vault above floor level.

The model includes a door at the maze entrance and an intermediate door in the middle of the maze. Both doors are a slab of 2.54 cm (1”) borated polyethylene. The entrance door also has a 0.3175 cm (⅛”) layer of lead on the outside. The air space in the maze above the 2.286 m (7 ½”) door height is filled with three air ducts surrounded by copper. Copper was chosen as an approximate model of the electric cables running through the space. The duct dimensions (25.4 cm [10”] wide by 53.45 cm [21”] high) were chosen so that the overhead space contains ½ air and ½ copper by volume.

The targets consist of a 75 µm havar foil over a vacuum tube leading to ^{18}O enriched water in a silver holder, all contained in an aluminum housing with a stainless steel backing plate. The collimator is modeled as a graphite block slightly offset from the target beam line.

B. Sources

The cyclotron produces a beam of 16.5 MeV protons. The maximum current used in the cyclotron room is 130 µA after a 10% loss upon passing through the collimator. The 130 µA is split between into 65 µA on two targets. For the Monte Carlo model, we use 130 µA on a single target. We also assume a fully irradiated (double) target emitting 2 x 3500 mCi of 0.511 MeV photons. The total (proton beam + photons) rate of particle emission is 8.927×10^{14} / second.

The target room model assumes a 80 µA proton beam impinging on the external target, a 8 µA beam loss on the collimator in the cyclotron room, and single 3500 mCi load of irradiated target material. The total rate of particle emission is 5.493×10^{14} / second.

Two proton beams are directed directed northward (to the right in Fig. 1) with a small divergence angle. The beam origins are just downstream of the respective target and the collimator. The photons are emitted isotropically. The photon source is distributed uniformly throughout the target water ($H_2\,^{18}O$) volume.

C. Mesh Tallies

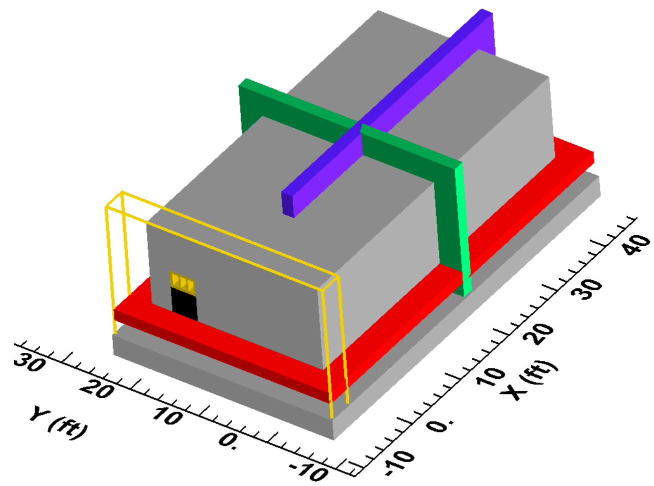

Fig. 2. Mesh tally locations in a 3-dimensional view.

Mesh tallies record the dose equivalent rate and its relative error (RE) on a spatial grid of mesh cells. Dose response functions were used to convert the flux to a dose rate. For neutrons, the response function was taken from NCRP-38 1971, ANSI/ANS 6.1.1—1977. The Quality Factors in the NCRP-38 dose response function match those listed in 10 CFR Part 20. For photons, the values in ICRP-21 1971 were used.

Four mesh tallies were used. They are shown in Figure 2. The horizontal red, north-south blue, and east-west green mesh tallies pass through the location of the cyclotron target. For external target irradiation, the green mesh tally is moved to pass through that target. The yellow (or tan) mesh tally covers the exterior of the south wall. This region is of interest because of the maze entrance and an operator's console east of (to the right in fig. 2) the entrance door.

Each mesh tally has one grid cell in the short direction (e. g. in the Z or up direction for the red horizontal tally) of length 50 cm (99 cm for the yellow south wall tally). The grid cell dimensions are 5 cm (10 cm for the south wall tally) in the other directions (e. g. X and Y for the red tally).

2. Preliminary Considerations

A. Proton Transport

The previous work enabled proton transport throughout the model. Some protons were scattered from the target and collimator, but very few of these reached the walls and ceiling. Secondary protons were produced by interactions within the concrete. Except in the target, collimator, and close surrounding air, the proton contribution to the dose equivalent rate was much smaller than the neutron and photon contributions. To verify that proton transport could be neglected in the concrete, we compared the results from two models with and without proton transport enabled within the walls and ceiling. The external neutron and photon dose rates were the same in both cases, showing that proton transport can be neglected in the SSR runs. The models with limited proton transport ran 1.7% and 16% more quickly under MCNPX and MCNP6, respectively.

B. MCNP6 & MCNPX Comparison

Our initial calculations with MCNP6 showed a much lower external neutron dose rate than with MCNPX. The discrepancy increased from the source through the walls. We traced the cause to the material definitions. Most material constituents were defined as elements in the initial models. When the elemental fractions were divided among the naturally occurring isotopes of the element, the MCNP6 and MCNPX results came into agreement. We used isotopic material definitions in succeeding models.

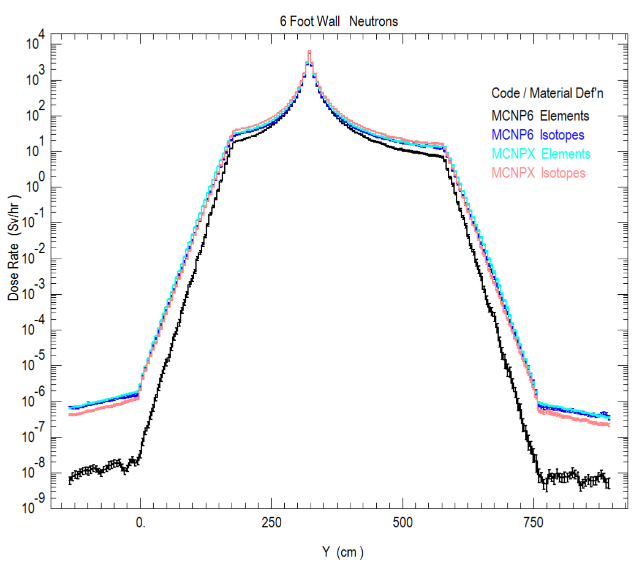

Fig. 3. Neutron dose equivalent rate from wall to wall through the cyclotron target for different options.

Figure 3 shows profiles of the neutron dose equivalent rate from wall to wall passing through the cyclotron target (bottom to top in Fig. 1) for the two codes using elemental and isotopic material definitions. All agree except for the MCNP6 model with elemental material definitions (black).

3. Surface Source Write

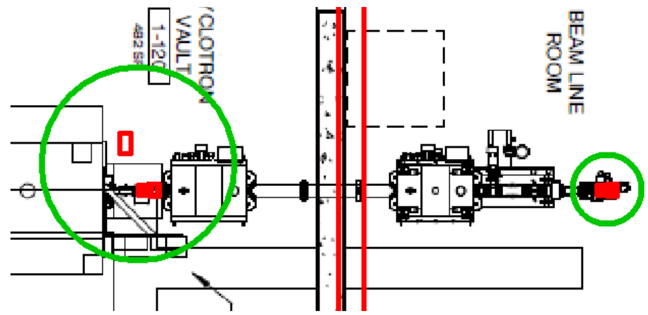

Fig. 4. Outlines of the target and collimator models (red) and surface source spheres (green) overlaid on the architectural drawing.

To take advantage of the multi-threading capability of MCNP6 when calculating a model transporting only neutrons and photons and to prepare sources for the ADVANTG code, we proceeded in two steps. In the first step, protons irradiated the target and collimator. The resulting neutrons and photons outwardly crossing a sphere surrounding the target(s) were saved to a file using the MCNP Surface Source Write (SSW) feature. Two SSW runs were made, one for each source location. Each followed 5×10^8 source protons. The cyclotron target SSW model included only the air in the room surrounding the target and collimator. The external target SSW model included air around the external target and collimator and a portion of the stub wall between the two rooms and wrote particles crossing both spheres. Figure 4 shows the location of the surface source spheres.

4. ADVANTG Models

The ADVANTG (AutomateD VAriaNce reducTion Generator) code from Oak Ridge National Laboratory calculates energy dependent WWs on a spatial grid covering the model. The WWs control the population of particles in the grid cells, ensuring a sufficient population for adequate sampling while preventing local over populations that increase computation time. The FW–CADIS (Forward-Weighted–Consistent Adjoint Driven Importance Sampling) method optimizes the WWs for low REs in each mesh tally cell. Except for the items noted here, default values were used for all options.

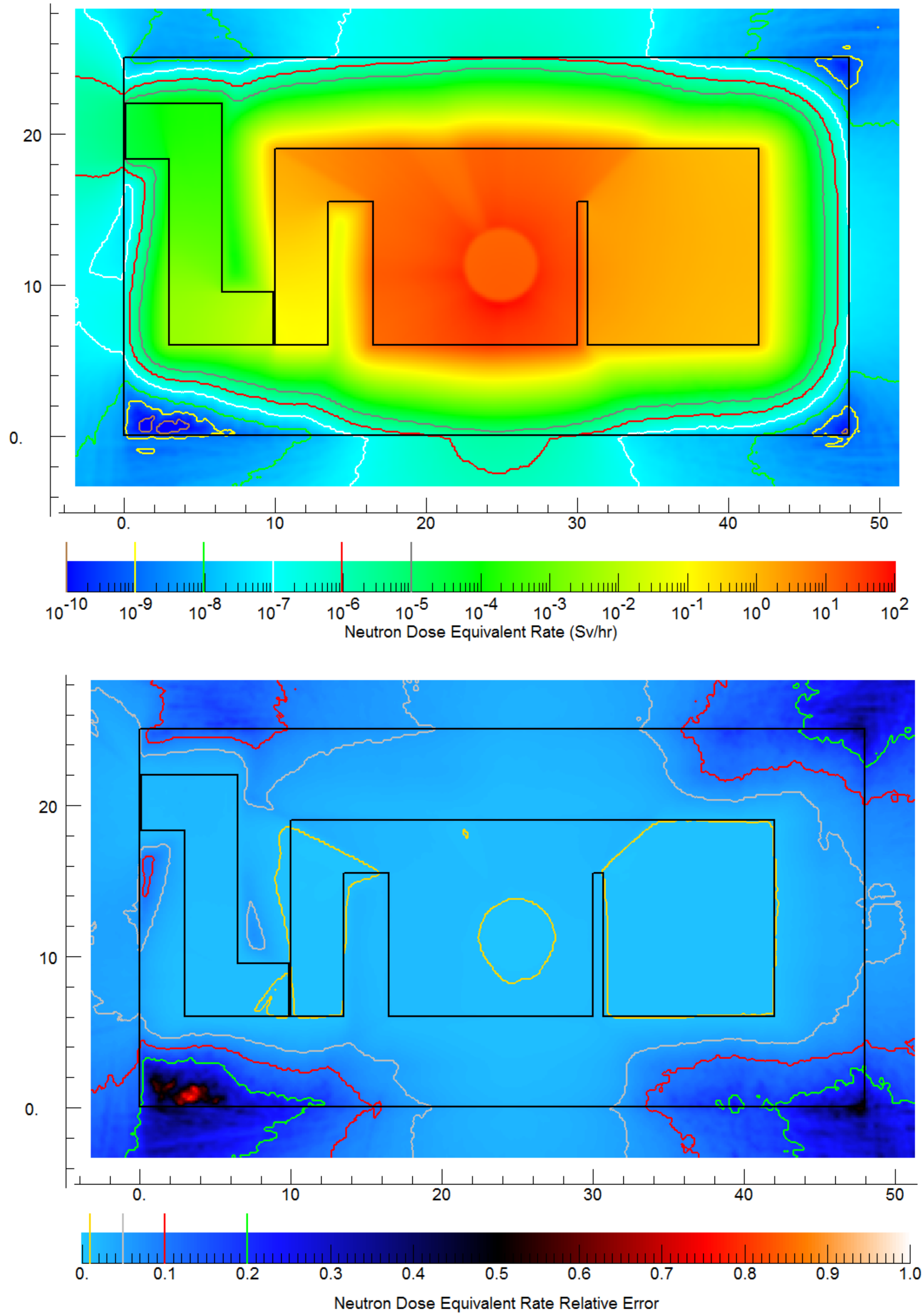

Fig. 5. Neutron dose equivalent rates (top) and relative errors (bottom). Dimensions are in feet.

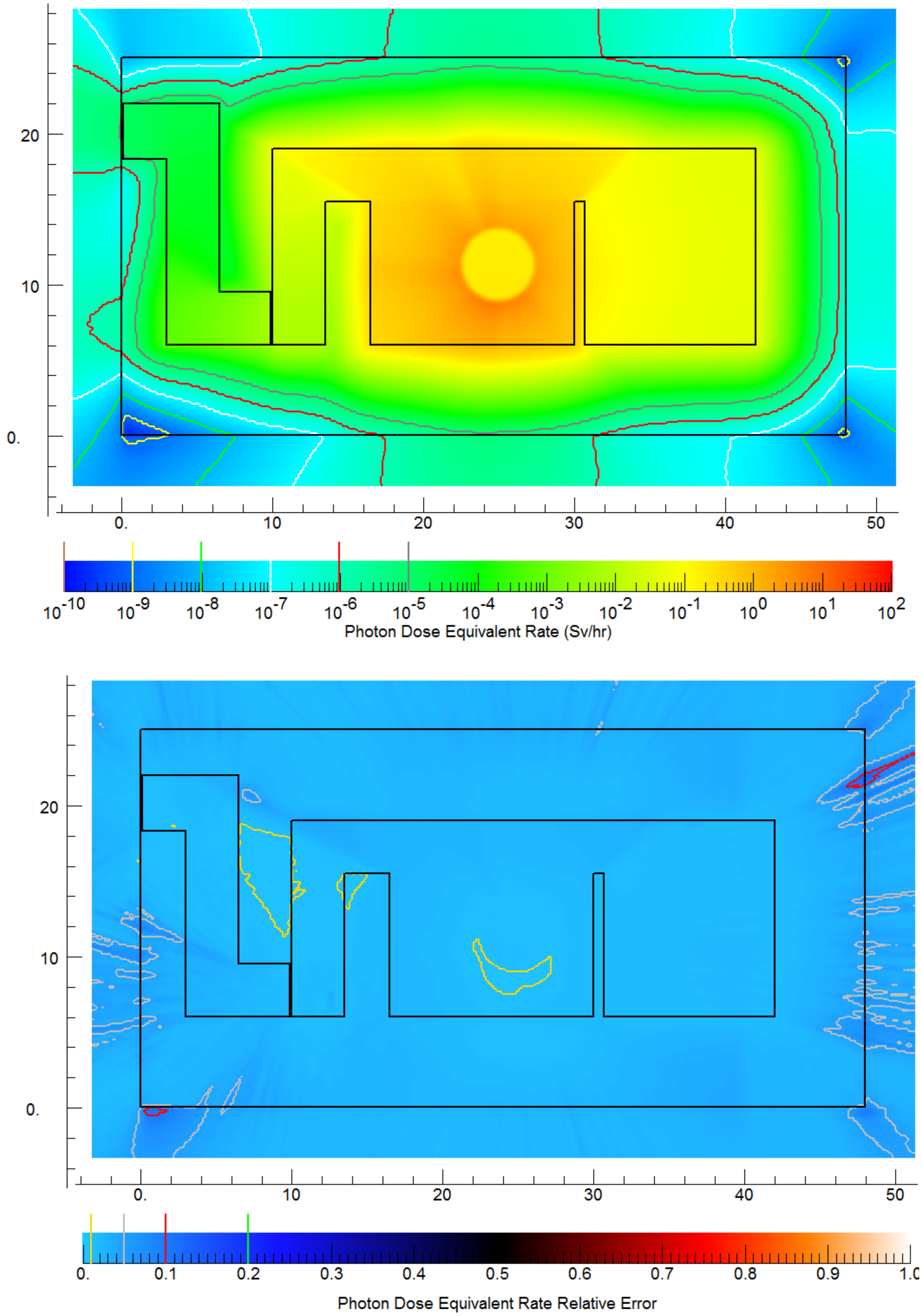

Fig. 6. Photon dose equivalent rates (top) and relative errors (bottom). Dimensions are in feet.

A, Spatial Grid

ADVANTG executes the Denovo discrete ordinates transport code on a Cartesian mesh overlaying the Monte Carlo model. We specified the grid using the X, Y, and Z plane coordinates of every plane in the Monte Carlo model, including the planes introduced previously for importance splitting. Except for the target models that are not used in the ADVANTG model, all geometry is defined by aligned planes. Because the Denovo grid contained all material boundaries, no mixed material cells were present.

B. Source Terms

Because the surface source is incompatible with ADVANTG, we converted neutron and photon surface tallies on a sphere(s) just outside of the surface source sphere(s) to a point source(s) at the center of the sphere(s). Each tally contained 200 energy bins. The point source weight for each component is the total value of the tally.

Comparison of test runs of the Monte Carlo model using the point source and the SSR source gave substantially identical results, showing that the point source was correctly defined and is adequate for use in the ADVANTG model.

C. Merging Weight Window Files

ADVANTG executes MCNP5 [5] to parse the Monte Carlo model. Because the MCNP5 source is restricted to a single particle type, a mixed neutron-photon source cannot be used. Instead, ADVANTG was run separately for neutrons and photons from the surface source. Separate ADVANTG calculations were made for irradiation of the cyclotron target and the external target.

The WWs are written to the file WWINP. The two WWINP files were manually merged with a text editor. The file consists of two header lines, the spatial grid, and then the WW data. The second line gives the number of neutron and photon energy bins. To merge, change the 0 for the number of photon energy bins in the neutron WWINP file to the value from the photon file, delete the header and spatial grid section from the photon file and append it to the neutron WWINP file. A comparison of the two files will show where the identical spatial grid section ends.

III. RESULTS

Four MCNP6 calculations using the ADVANTG WWs were made: with and without an intermediate maze door for each of the cyclotron and external target sources. Figures 5 and 6 show the neutron and photon dose equivalent rates and REs in the horizontal mesh tally for the cyclotron target model with the intermediate door. Except for small regions of low neutron dose rate near the vault corners, all REs are ≤ 0.1, indicating valid results. The other models gave similar good results. The linear regions of higher photon RE at the left and right edges are due to a small number of high energy source photons.

Reading once through the SS file resulted in the processing of 3.3×10^{6} histories requiring approximately 12 hours of wall clock time when running with 14 threads. A comparison run using importance splitting, rather than the ADVANTG WWs, was terminated after 6 days of running with 40 threads, having processed only 0.85×10^{6} histories. Similar dose rates obtained but with much larger REs. Figure 7 compares the cumulative photon and neutron REs for each of the variance reduction methods. The curves show the fraction of mesh tally cells with REs less than or equal to the RE on the abscissa. The default output from the SSR runs does not list the Figure of Merit (FOM), so a comparison of the FOMs is not possible.

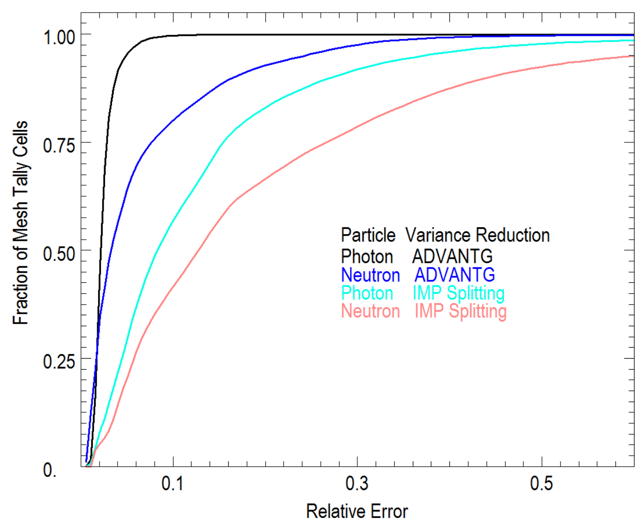

Fig. 7. Fraction of mesh tally cells with RE less than or equal to the RE on the abscissa.

A. Attenuation Through the Doors

Figure 8 shows the total, neutron, and photon dose equivalent rates along a south to north path passing through the center of the intermediate door position (x = 10 feet). Two sets of curves compare the profiles with and without the 2.54 cm borated polyethylene door for irradiation of the cyclotron target. The total and neutron dose rates drop by a factor of 5 passing through the intermediate door. The door does not attenuate the photon dose. Similar reductions obtain for external target irradiation.

Neutrons dominate the total dose equivalent rate in the interior of the vault. The steep decline between x = 3 feet and x = 0 occurs in the southernmost concrete barrier. Photons dominate the total dose equivalent rate exterior to the vault.

Figure 9 shows the total, neutron, and photon dose equivalent rates along a south to north path passing through the center of the entrance door (x = 0) for the case of cyclotron target irradiation with an intermediate door. The neutron, photon, and total dose rates decrease by factors of 7, 2, and 3.5, respectively, through the entrance door. Similar reductions obtain for external target irradiation and in the models without an intermediate door.

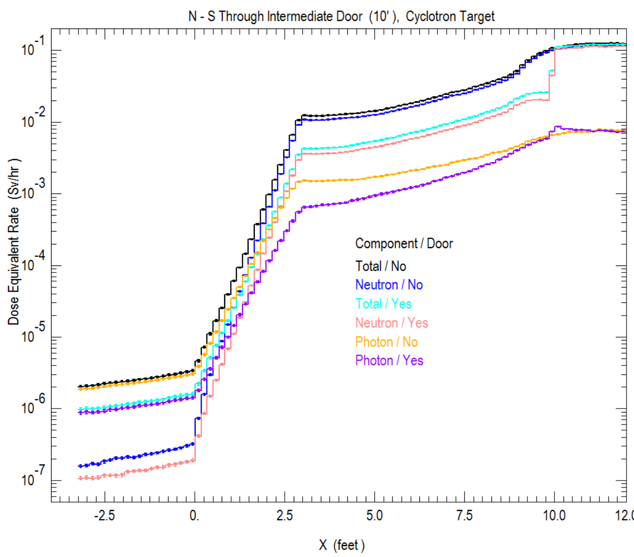

Fig. 8. Dose equivalent rate profiles along a south-north path through the intermediate door position.

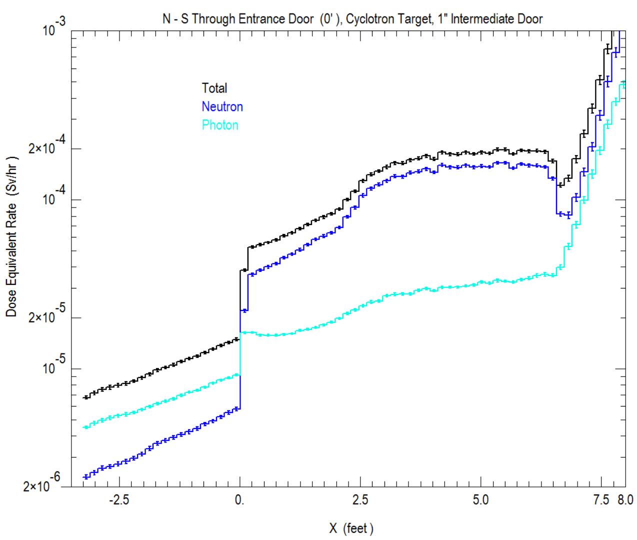

Fig. 9. Dose equivalent rate profiles along a south-north path through the entrance door.

B. Dose Equivalent Rates Exterior to the South Wall

The operators' console is located exterior to the south wall to the east of the entrance door. The south mesh tally (yellow-tan in figure 2) covers the console location and the exterior of the entrance door and the air ducts above the maze. Figure 10 shows the neutron (top) and photon (bottom) south mesh tallies for the beam on cyclotron target with the intermediate door. The horizontal and vertical black lines outline the extent of the vault, the entrance door, and the duct space above the door. All photon REs are ≤ 0.1. The neutron REs are ≤ 0.1 in regions where the dose rate is > 5×10^{-8} Sv/hr. Neutron REs slightly exceed 0.2 in the region beyond the vault boundary at the right of the figure.

The air ducts do not contain any barriers equivalent to the doors in the maze. The radiation flow through the smaller ducts is much less than through the maze, as is the dose rate exterior to the ducts and the maze.

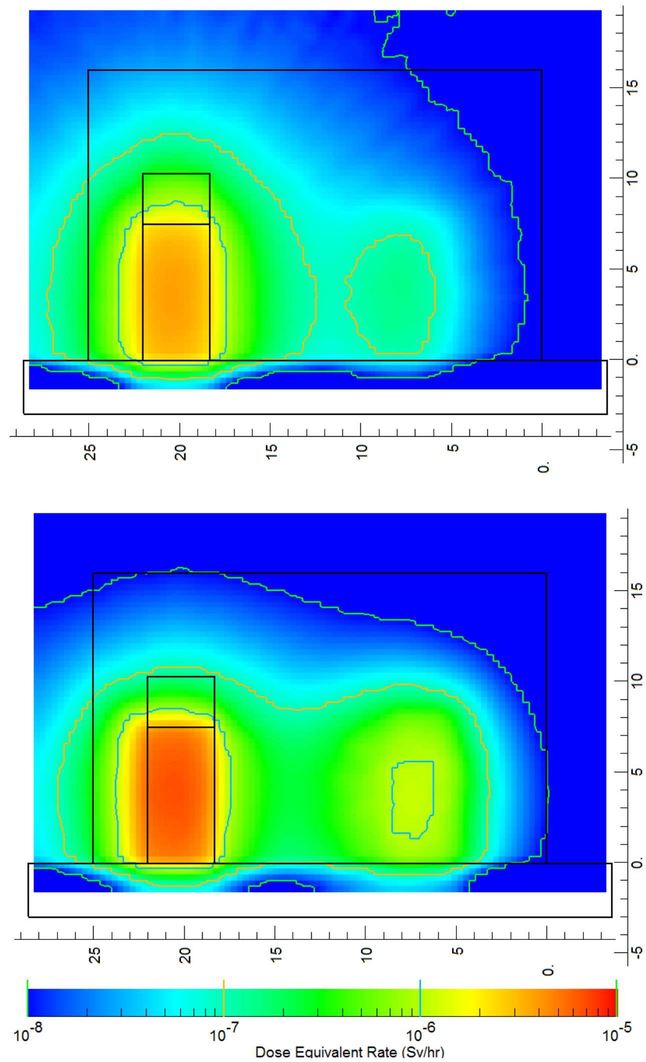

Fig. 10. Neutron (top) and photon (bottom) dose equivalent rates exterior to the south wall. Dimensions are in feet.

The secondary peak to the right of the door results from the penetration of the south wall opposite the north-south leg of the maze. The intermediate door decreases the intensity of the secondary peak as well as the dose rate at the entrance. Figure 11 shows profiles of the total dose equivalent rate from east to west (right to left in fig. 10) at ½ the maze height in the south mesh tally. Results are from all 4 models (cyclotron/external target with and without the intermediate door) considered. The intermediate door results in a factor 2 reduction in the external dose rate at both the entrance and the secondary peak.

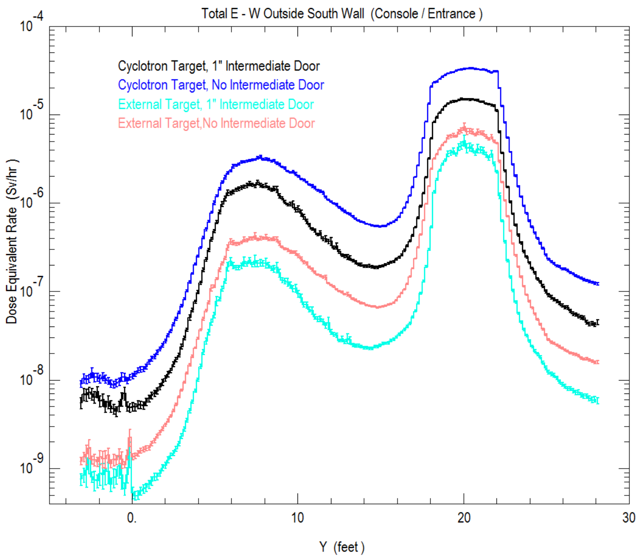

Fig. 11. Total dose equivalent rate profiles along an east to west path exterior to the south wall.

IV. CONCLUSIONS

We have successfully applied WWs calculated by ADVANTG to a model with a proton beam source. The use of these WWs resulted in a significant reduction of MCNP6 calculation time, even with the additional steps required, compared with variance reduction by importance splitting. The resulting small errors permit meaningful comparisons of the external dose equivalent rates among the different models studied.

ACKNOWLEDGMENT

We thank the cyclotron team at the Jacksonville Florida campus of the Mayo Clinic for their support of this work.

REFERENCES

1. K. A. VAN RIPER, R. L. METZGER, and K. NELSON, "Shielding Design of the Mayo Clinic Scottsdale Cyclotron Vault," *Proc. Joint 13th International Conference on Radiation Shielding & 19th Topical Meeting of the Radiation Protection and Shielding Division of the ANS ICRS-13 & RPSD-2016,* Paris, France, October 3-6, 2016.
2. D. PELOWITZ (ed.), "MCNPX User's Manual, Version 2.7.0," Los Alamos National Laboratory, LA–CP–11–00438 (2011).
3. D. B. PELOWITZ, A. J. FALLGREN, G. E. MCMATH. "MCNP6 User's Manual, Code Version 6.1.1beta," Los Alamos National Laboratory, LA–CP–14–00745, Rev. 0, (2014).
4. W. MOSHER, et. al, "ADVANTG - An Automated Variance Reduction Parameter Generator," ORNL/TM–2013/416 Rev. 1, Oak Ridge National Laboratory, Oak Ridge, TN, (2015).
5. Los Alamos Monte Carlo Group, "MCNP-A General Monte Carlo N-Particle Transport Code Version 5," Vols. I-III, Los Alamos National Laboratory, LA-UR-03-1987 (2003).